Fractional Order Control of Micro Electro-Mechanical Systems

Mohammad Goodarzi[1*]
[1]Department of Electrical Engineering, Faculty of Engineering, Garmsar Branch, Islamic Azad University, Garmsar, Iran
[*]Email of corresponding author: m_goodarzi181@yahoo.com
Received: June 28, 2016; Accepted: September 13, 2016

Abstract
This paper addresses the problem of the fractional sliding mode control (FSMC) for a MEMS optical switch. The proposed scheme utilizes a fractional sliding surface to describe dynamic behavior of the system in the sliding mode stage. After a comparison with the classical integer-order counterpart, it is seen that the control system with the proposed sliding surface displays better transient performance. The claims are justified through a set of simulations and the results obtained are found promising. Overall, the contribution of this paper is to demonstrate that the response of the system under control is significantly better for the fractional-order differentiation exploited in the sliding surface design stage than that for the classical integer-order one, under the same conditions.

Keywords
Fractional Order Control, Sliding Mode, Micro-Electro Mechanical Systems (MEMS), Lyapunov Stability, Robust Control

1. Introduction

Micro-Electro-Mechanical-Systems are emerging systems with ever-increasing applications in modern industries. MEMS technology can be utilized to produce complex structures, devices and systems in the micrometer scale [1-2]. They have enabled many types of sensors, actuators and systems to be reduced in size by several orders of magnitude, while at the same time improved their performances [3]. One of the fields that undergo rapid miniaturization is that of optical signal transmission [4]. Bandwidth is limited by large-scale matrix switches, requiring signal conversion from optical, to electronic, and reverse. One solution to this problem is utilizing MEMS optical switches to perform switching operations. MEMS optical switches manipulate optical signals directly, without first converting them to electronic signals with lower size and power consumption [5]. This is important whereas telecommunication industry desire to focus on all-optical networks, meaning total exclusion of signal conversion in optical signal transmission.

The considerable point is that, although, the advances in micromachining technology make it possible for large-scale matrix switches to be monolithically integrated on a single chip [6], there are yet several problems.

MEMS models suffer from nonlinearities and uncertainties like many other dynamical systems.

Unlike macro mechanical systems where the dynamic modeling is relatively simple, it is quite problematic in the MEMS case. Damping rate is the parameter, which is difficult to determine analytically, even through finite element analysis [7]. The presence of high-frequency system

dynamics is also introduced as additional challenge for the MEMS dynamic modeling that increases the systems' complexity and so invokes appropriate controllers to cope with this issue.

A lot of researchers have focused on some possible solutions to overcome the aforementioned weaknesses [4, 8-18]. Considering the earlier works, it shows that, almost, sliding mode control has been received more and more attention, recently. Sliding mode control design is believed to be robust with respect to system uncertainties in both theoretical research and application. It combines the intuitive nature of feedback linearization control with the robustness of sliding mode techniques in the controller design phase. This type of control design has several interesting and important properties that cannot be easily obtained by other approaches. When a system is in the sliding mode, it emulates a prescribed reduced-order system and is insensitive to parameter variations and disturbance. Precise dynamic models are not required and the control algorithms are easy to implement. All these properties make the sliding mode control an ideal candidate for MEMS control.

As a result, in the related literature, the absence of methods designed and implemented via fractional differentiation in robust and nonlinear control is visible.

The purpose of this paper is to fill this gap to the extent that covers the following: 1) better transient performance than those utilizing traditional integer-order operators; 2) employing additional design options; 3) conditions for hitting in finite time and 4) sliding mode control based on fractional order differentiation. This paper addresses the issue of SMC of a MEMS optical switch in the presence of parametric uncertainty. Toward this end, a sliding surface is used to describe dynamic behavior of the system in the sliding mode stage. A control scheme is then derived to govern the motion of the under control system such that it converges to the ideal manifold. Based on this control scheme, a fractional form of sliding mode control strategy is proposed for the case of uncertain parameters. The stability of the system is demonstrated using Lyapunov theory.

This paper is organized as follows. In section 2, we recall some basic relationships for describing fractional order calculus. Section 3 describes the dynamic equation and the property of MEMS dynamic parameters. The plant parameters are assumed to be uncertain, but with known upper and lower bound, in this section. In section 4, the traditional SMC problem is proposed and the control input is designed. The fractional sliding mode control scheme derivation and stability analysis are then presented. Section 5 shows the robust performance of both SMC/FSMC from the simulation results, which is followed by conclusion in section 6.

2 Fractional Calculus

In this section, some basic definitions related to fractional calculus are presented. In fractional calculus, the traditional definitions of the integral and derivative of a function are generalized from integer orders to real orders. In the time domain, the fractional order derivative and fractional order integral operators are defined by a convolution operation.

Several definitions exist regarding the fractional derivative of order $\alpha \geq 0$, but the Caputo definition in (1) is used the most in engineering applications, since this definition incorporates initial conditions for $f(t)$ and its integer order derivatives, i.e., initial conditions that are physically appealing in the traditional way.

Definition 1 (Caputo fractional derivative [19]). The Caputo fractional derivative of order $\alpha \in \Re^{+}$ on the half axis $\Re^{+}$ is defined as

$$f(t)=\frac{1}{\Gamma(n-\alpha)}\int_{a}^{t}\frac{f^{(n)}(\tau)}{(t-\tau)^{\alpha-n+1}}d\tau. \quad t>a \tag{1}$$

With $n=\min\{k \in \square / k>\alpha\}, \alpha>0$, and $\Gamma(n)$ denoting the famous Gamma function, which is defined as

$$\Gamma(n)=\int_{a}^{\infty}t^{n-1}e^{-\tau}d\tau \tag{2}$$

For the Caputo derivative, we have

$$D_{t}^{\alpha}\sigma=0, \quad (\sigma \text{ is a constant}) \tag{3}$$

Nonlinear dynamic description is studied in the next section.

3. Dynamic Modeling

The scanning electron microscope (SEM) micrograph of the MEMS optical switch composed of an electrostatic comb drive actuator, a suspension beam, and reflection micromirror with optical fiber grooves is shown in Figure 1. Optical fibers will be inserted into the fiber grooves and deliver the light from one input to another output. Without external voltage, the mirror is in the beam path and the incident signal from input fiber is reflected by the mirror into the output fiber, the switch is at the cross state. When the actuator is applied by a proper driving voltage, the electrostatic force induced by the actuator will drive the shuttle and so the attached micro mirror out of the beam path. As a consequence, the incident beam will be transmitted directly into the other output fiber, where the switch is at bar state. When the voltage is released, the mirror will latch to the original position and the cross state is recovered [5]. In order to obtain the dynamic equations of MEMS optical switch, one needs to determine all forces, electrostatic and mechanical, acting on the shuttle. It is assumed that, the shuttle has one degree of freedom and other situations, for instance, rotation around the main body axes, translational along them, as well as different vibration modes that impose additional degrees of freedom are not considered here. Finally, the optical model will be achieved. We will perform this derivation in three steps.

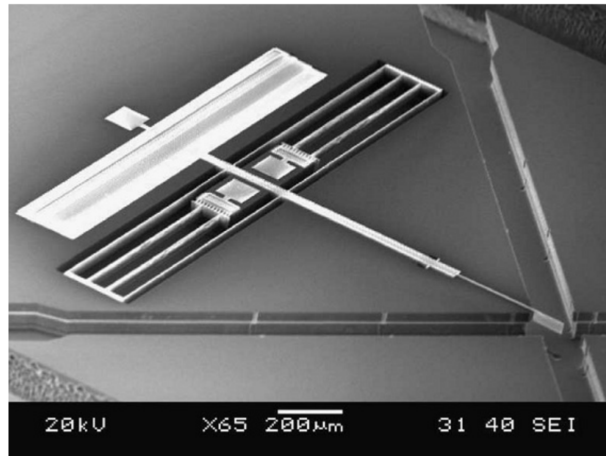

Figure1. SEM image of a MEMS optical switch [5]

Step1: In order to obtain the model of electrostatic force between the two comb drive electrodes, first the capacitance of the comb drive should be determined as a function of position. The capacitance is calculated as a sum of parallel capacitances among pairs of comb electrodes. The total capacitance, as a function of the position x , is given as [5, 12]

$$C(x) = \frac{2n\varepsilon_0 T(x + x_0)}{d} \tag{4}$$

Where n is the number of the movable comb fingers, $\varepsilon_0 = 8.85\times10^{-12} F/m$ is the permittivity or dielectric constant for free space, T and d are the thickness of the finger and the gap between fingers, respectively, x is the shuttle position, and x_0 is the initial overlapping between the electrodes. The electrostatic force between the electrodes of the capacitor is then given by [7, 12]

$$f(v, x) = \frac{1}{2} v^2 \frac{\partial C}{\partial x} \tag{5}$$

Substitute the total capacitance denoted by (4) into (5) to get the following relation for the electrostatic force:

$$f(v, x) = \frac{n\varepsilon_0 T}{d} v^2 = k_e v^2 \tag{6}$$

Where k_e is the input gain and v denotes the voltage applied over terminals of the comb drive electrodes.

Remark 1: The electrostatic force depends only on the voltage across the capacitor not on the position. It returns to the linearity between the capacitance and the position over a wide range of deflections that is the most important characteristics of the comb drive.

Step2: Here, we will obtain mechanical forces imposed to the shuttle. It consists of two elements. The first one is the so-called stiffness of the suspension mechanism, and the second one is a function describing losses such as damping and friction. As mentioned before, damping is the most difficult parameter to determine analytically, even through finite element analysis (FEA). The

reason lies in the number of different mechanisms that causes it, including friction, viscous forces, drag, etc [7]. Generally, they can be defined as [4]

$$d(x,\dot{x}) = \frac{\eta}{2\varepsilon_0} C(x)\dot{x} = (d_x x + d_0)\dot{x} \qquad (7)$$

Where η is velocity of the air surrounding switch.

Now, according to the last steps, and utilizing the Newton's second law, the motion equation of the MEMS optical switch is obtained as

$$m\ddot{x} = k_e v^2 - d(x,\dot{x}) - k_x x \qquad (8)$$

Where $m = m_{mirror} + 0.5 m_{rigid} + 2.74 m_{beam}$ is the effective moving mass of the shuttle. For the purpose of convenience of controller design procedure, let $y = [y_1 \quad y_2]^T = [x \quad \dot{x}]^T$. Then (7) can be rewritten as

$$\begin{cases} \dot{y}_1 = y_2 \\ \dot{y}_2 = N(y_1, y_2) + gu \end{cases} \qquad (9)$$

Where

$$N(y_1, y_2) = -\frac{1}{m}(d(y_1, y_2) + k_x y_1) \quad , \quad g = \frac{k_e}{m} \qquad (10)$$

And $u = v^2$ will be referred to as the control signal.

Step3: Here, we will achieve the optical model for MEMS optical switch. It is simply a function that connects the intensity of light to the position of the blade, as shown in Figure 2. The light beam is intercepted by the blade, increasing and decreasing the through put of light. The Rayleigh-Somerfield model is based on a Gaussian distribution of the intensity across the light beam. The waist of the Gaussian beam coming from the fiber is w_0. As the beam propagates in free space the waist w_1 is given as

$$w_1 = w_0 \sqrt{1 + \left(\frac{z_1}{z_R}\right)^2} \quad , \quad z_R = \frac{\pi w_0^2}{\lambda} \qquad (11)$$

With $w_0 = 5.1 \mu m$, $z_1 = 10 \mu m$ and $\lambda = 1.55 \mu m$. The transmitted power can then be described as

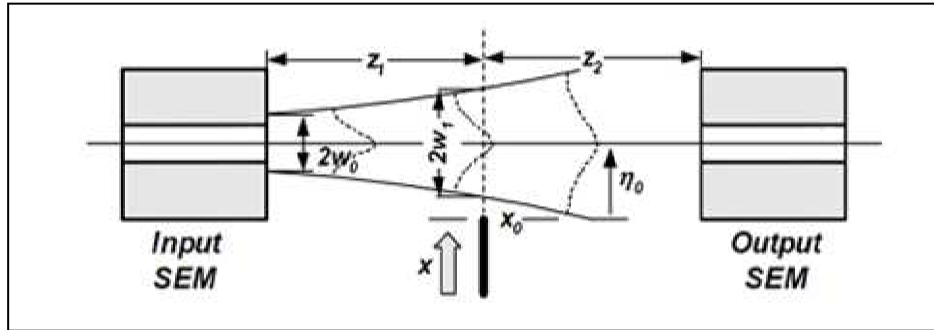

Figure2. Optical model [5]

$$P = h(x) = 0.5\left(1 - erf\left(\frac{\sqrt{2}(x - \eta_0)}{w_1}\right)\right) \tag{12}$$

Where η_0 denotes the distance from the fiber axis. For a good survey, the reader may study [12]. In summary, the complete dynamic equations of the MEMS optical switch can be described by (7) and (12). The terms of such a dynamical model satisfy some properties as mentioned in ref [15].

4. Robust SMC design

In this section, first considering uncertainties in the MEMS model, a robust sliding mode controller is proposed. Second, its robust stability is analyzed with respect to the model uncertainties. Finally, we discuss the conditions for fractionally amalgamated sliding mode control to stabilize the global under controlled system. Toward this end, suppose that $N(y_1,y_2)$ is the lumped sum of nonlinearities given by

$$N(y_1, y_2) = N_m + \Delta N \tag{13}$$

Where N_m denotes the mean value of the corresponding $N(y_1, y_2)$, and ΔN is the mismatch between the actual and estimated stiffness and damping terms. Furthermore, a multiplicative model is chosen for the control gain function g as

$$g = g_{\mathrm{m}} \Delta g \tag{14}$$

With g_m denoting nominal value of g . The following assumption turns out to be crucial within the analytical setting considered in this work.

Assumption 1: The terms on damping and stiffness are assumed to be bounded by some known function $\rho(y_1, y_2, t)$ as

$$\left|\Delta N\right| \le \rho(y_1, y_2, t) \quad \forall y_1, y_2 \in \square \tag{15}$$

Assumption 2: The control gain function satisfies:

$$0 < \gamma_{\min} = \frac{\underline{k}_e}{g_{\mathrm{m}}\overline{m}} \le \Delta g \le \frac{\overline{k}_e}{g_{\mathrm{m}}\underline{m}} = \gamma_{\max} \tag{16}$$

Where $\gamma_{\min}$ and $\gamma_{\max}$ are real positive constants.

Assumption 3: The desired trajectory signals y_{1d} , and $\dot{y}_{1d}$ are bounded by Y_M , and V_M respectively, i.e.,

$$Y_M = \sup_t |y_{1d}| \quad , \quad V_M = \sup_t |\dot{y}_{1d}| \tag{17}$$

4.1 Traditional SMC design

Consider the dynamic equations of the MEMS optical switch given by Equation (8). Let

$$y_{2d}(t) = \dot{y}_{1d}(t) \quad , \quad y_d(t) = \begin{bmatrix} y_{1d}(t) & y_{2d}(t) \end{bmatrix}^T \tag{18}$$

Define error function as

$$e(t) = y(t) - y_d(t) = \begin{bmatrix} e_1(t) \\ e_2(t) \end{bmatrix} = \begin{bmatrix} e_1(t) \\ \dot{e}_1(t) \end{bmatrix} \tag{19}$$

Where $e_1(t)$ denotes position error, and $e_2(t)$ represents velocity error. The sliding mode control u is characterized by the control structure defined by

$$u = \begin{cases} u^+(e) & \text{for } s(e) > 0 \\ u^-(e) & \text{for } s(e) < 0 \end{cases} \tag{20}$$

Where $s(e)$ is a switching function and defined as

$$s(e) = \dot{e}_1(t) + \Gamma e_1(t) = 0 \tag{21}$$

Where Γ is a constant to be determined. The design of sliding mode control involves two phases. The first phase is to select the switching hyper plane $s(e)$ to prescribe the desired dynamic characteristics of the controlled system. The second phase is to design the discontinuous control such that the system enters the sliding mode $s(e) = 0$ and remains in it forever. The interested reader is referred to the works of [20-21] for complete details on the historical aspects of the approach and its wide range of applications. When in sliding, the system satisfies

$$s(e) = 0 \quad , \quad \dot{s}(e) = 0 \tag{22}$$

And the system exhibits invariance properties, yielding motion independent of certain parameter variations and disturbances [22]. From the equations in (17), one can see that

$$\dot{s}(e) = N_m + \Delta N + g_{\mathrm{m}} \Delta g u - \dot{y}_{2d}(t) + \Gamma e_2(t) = 0 \tag{23}$$

And the equations governing the system dynamics may be obtained by substituting a so-called equivalent control, denoted by u_{eq} , for the original control u

$$u_{eq} = \frac{1}{g_{\mathrm{m}}}(-N_m + \dot{y}_{2d}(t) - \Gamma e_2(t)) \tag{24}$$

Such that under the control the dynamics in the sliding mode becomes

$$\dot{y}_2 = N + \Delta g(-N_m + \dot{y}_{2d}(t) - \Gamma e_2(t)) \tag{25}$$

It must be noted that, existence of (19) constitutes a necessary condition for the certain of a sliding motion on the sliding surface. A necessary and sufficient condition for the existence of a sliding regime on $s(e)$ is that the well-known existence condition $s\dot{s} < 0$ be satisfied. As a consequence of this, the control algorithm implements a set of decision equations so that a control action forces the MEMS to match the reference model (16). The control vector that satisfies the existence conditions obeys a law of the type

$$u_r = -\kappa sgn(s) \tag{26}$$

In which κ is a scalar design parameter that will be used later to prove stability of control system and *sgn* represents the sign function.

Proof: To study the stability of the origin of the state space, we use Lyapunov's direct method by proposing the following Lyapunov function candidate

$$V(s) = \frac{1}{2}s^2 \tag{27}$$

Differentiating (22) along equation (18) with equations (19) and (21),

$$\dot{V}(s) = s\dot{s} = s\left((1-\Delta g)\left(N_m - \dot{y}_{2d}(t) + \Gamma e_2(t)\right) + \Delta N - \kappa g sgn(s)\right) \tag{28}$$

Using the assumptions 1 and 2,

$$\dot{V}(s) \le |s|\left((1-\gamma_{\min})\left|N_m - \dot{y}_{2d}(t) + \Gamma e_2(t)\right| + \rho(y_1, y_2, t) - \kappa \underline{g}\right) \tag{29}$$

Thus, the sufficient condition to establish $\dot{V}(s) \le 0$ is

$$\kappa > \underline{g}^{-1}\left((1-\gamma_{\min})\left|N_m - \dot{y}_{2d}(t) + \Gamma e_2(t)\right| + \rho(x_1, x_2, t)\right) \tag{30}$$

Remark 2: As it can be seen from (15), a discontinuous sliding reachability condition is used to eliminate deviations from the sliding surface in the presence of uncertainty. However, in practice, due to the finite switching time, the frequency is not infinity high. The control is discontinuous across the switching surface and chattering takes place. A common approach to reduce chattering is to introduce a boundary layer, ε, around the sliding surface to use a continuous sliding reachability condition within the boundary layer. Using a saturation function $\mathrm{sat}_\varepsilon(\mathrm{s})$ instead of $sgn(s)$ in controller design will reduce chattering. The term $\mathrm{sat}_\varepsilon(\mathrm{s})$, with a saturation limit $\varepsilon > 0$, is defined by

$$\mathrm{sat}_\varepsilon(\mathrm{s}) = \mathrm{sat}\left(\frac{\mathrm{s}}{\varepsilon}\right) = \begin{cases} 1, & \mathrm{s} > \varepsilon \\ \mathrm{s}/\varepsilon, & |\mathrm{s}| \le \varepsilon \\ -1, & \mathrm{s} < -\varepsilon \end{cases} \tag{31}$$

Thus, equation (21) is replaced by

$$u_r = -\kappa sat\left(s/\varepsilon\right) \tag{32}$$

This completes stability proof for control design

4.2 Fractional SMC design

In the sliding mode controllers for MEMS proposed so far, the MEMS dynamic is constrained to follow a first order model as (16). This is not the only possible structure, and other designs with more complex or time-varying surfaces may provide potential advantages. As a result, in the related literature, the absence of methods designed and implemented via fractional differentiation in robust and nonlinear control is visible.

Consider the MEMS system (8) with the following choice of sliding surface to define dynamic behavior of system in sliding mode

$$s(e) = D_t^{\alpha} e_1 + \Gamma e_1 \tag{33}$$

It must be noted that Γ is designed such that the sliding mode on $s(e)=0$ is stable, i.e., the convergence of s to zero in turn guarantees that e_1 also converges to zero. Any positive scalar Γ will satisfy this condition.

Theorem: The MEMS optical switch given by (8) with the switching surface (28) is Uniformly Ultimately Bounded (UUB) by applying the control law

$$u = \frac{1}{g_{\mathrm{m}}}\left(-N_m + D_t^{1-\alpha}\left(D_t^{1+\alpha} y_{1d}(t) - \Gamma e_2(t)\right)\right) - \kappa sgn(s) \tag{34}$$

Where the parameters are defined as before.

Proof: The proof is the same as in section 4.1. To do so, the same lyapunov function candidate (22) is considered. Let us differentiate s with respect to time once to make u appear.

$$\dot{s}(e) = D_t^{1+\alpha} e_1 + \Gamma e_2 \tag{35}$$

By differentiating the Lyapunov function candidate (22) with respect to time, and using Equations (29) and (30), we obtain

$$\begin{aligned}\dot{V}(s) &= s\left(D_t^{\alpha-1}(N+gu) - D_t^{1+\alpha} y_{1d}(t) + \Gamma e_2\right)\\ &= s\left(D_t^{\alpha-1}\left(N - \Delta g N_m\right) + (\Delta g - 1)\left(D_t^{1+\alpha} y_{1d}(t) - \Gamma e_2\right) - D_t^{\alpha-1}\kappa g sign(s)\right)\end{aligned} \tag{36}$$

Similarly, since Eq. (31) must be negative definite, therefore, by choosing the control parameters as

$$\kappa > \max\left|\underline{g}^{-1} D_t^{1-\alpha}\left(D_t^{\alpha-1}\left(N - \Delta g N_m\right) + (\Delta g - 1)\left(D_t^{1+\alpha} y_{1d}(t) - \Gamma e_2\right)\right)\right| \tag{37}$$

Uniform Ultimate Boundedness of the switching variable $s(e)$ thus follows using the results of equation (32). Therefore all variables are bounded, and the switching variable $s(e)$ will converge to

zero, and the stability of the switching surface guarantees that the tracking error will also converge to zero.

5. Simulation results

The performance robustness of proposed controller is verified through simulations against the parameter uncertainty. The MEMS optical switch is assumed to be driven by a uni-polar voltage source, which its amplitude is limited by a saturation block to 0 and 35 volt. Table I shows the nominal values of its physical parameters. The performance of the proposed controller is compared with that of the robust traditional SMC method. It is assumed that the uncertain values of the mass, stiffness, damping and friction are 20% higher than the measured. The controller parameters are set as $\kappa = 10^{-7}$, $\Gamma = 2$, and $\alpha = 0.7$. Fig. 3 shows the system response for short displacement of actuator, for both SMC and FSMC. As it can be seen, the output signal converges to the desired set point well and there are no oscillations. FSMC has a faster time response than traditional SMC due to having additional control parameters in research space. Fig.4 shows the actual control input. As it is shown in Fig. 5, the sliding motion starts at a point and the tracking error then approaches the origin by a spiral trajectory. Hence, it is straightforward to draw the conclusion that the system under control is potentially stable by choosing suitable control parameters satisfying the conditions (25) and (32) even in the presence of system uncertainties.

Table1. The MEMS parameters

$k_x = 0.6 \pm 0.12\ Nm^{-1}$	$d_x = 0.0363 \pm 0.00726$	$d_0 = (4.5 \pm 0.9) \times 10^{-3}\ Ns$
$k_e = (1.9 \pm 0.38) \times 10^{-8}\ N/V^2$	$m = 2.35 \times 10^{-9} kg$	$d = 2.6 \mu m$

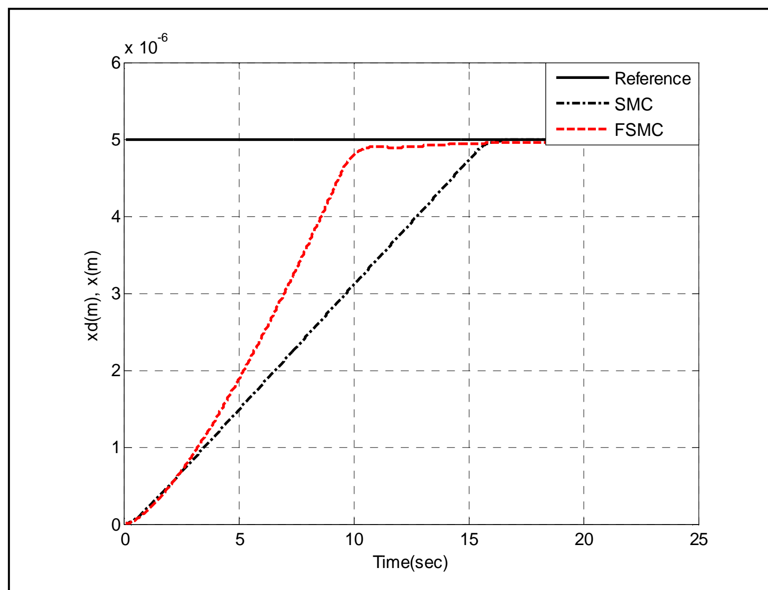

Figure3. Responses of the system to $x_d = 5\mu m$

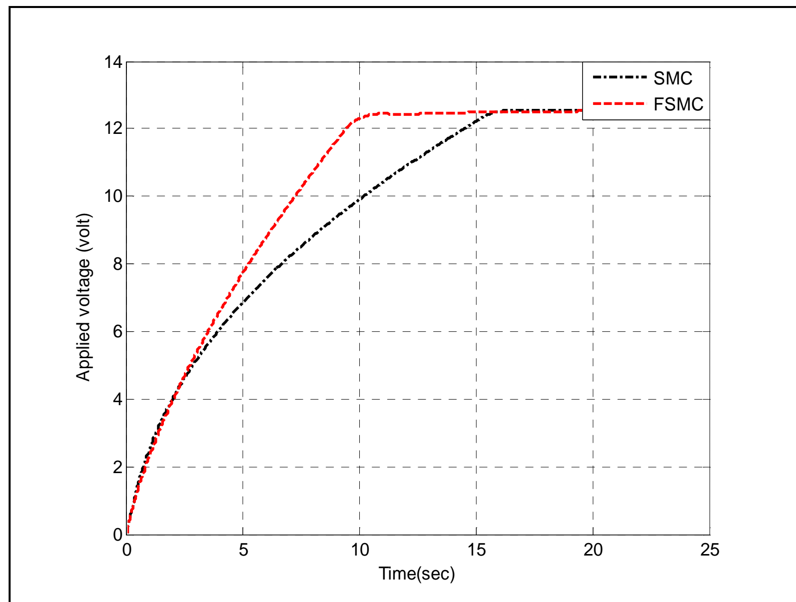

Figure4. Input voltages

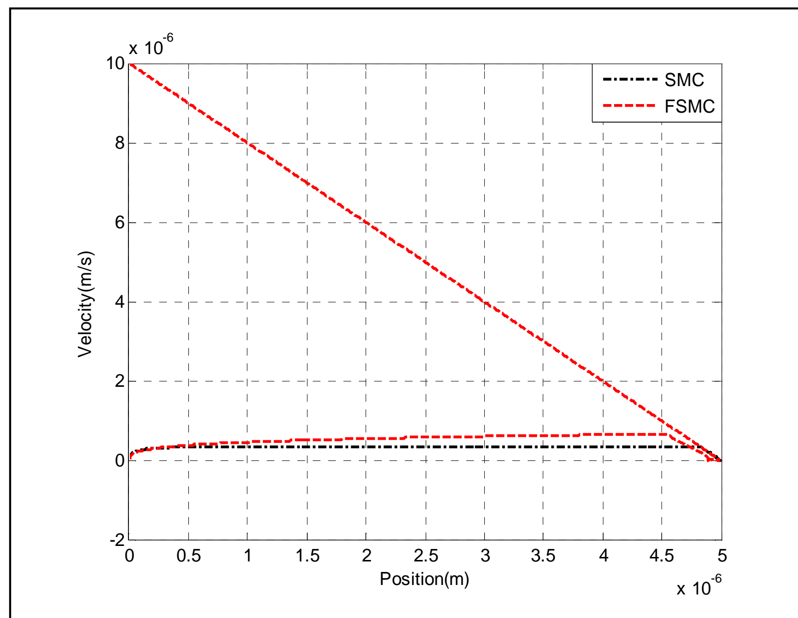

Figure5. Phase plane trajectories for the MEMS under SMC and FSMC

6. Conclusion

A Robust sliding mode controller is proposed to overcome uncertainties of MEMS optical switches, and to guarantee boundedness of the tracking errors. It is assumed that in dynamic equations of the system, all the terms are uncertain and only some information about their upper/lower bounds is available. The system stability was verified analytically. It was shown that by choosing control parameters properly, the uniformly ultimately boundedness stability is guaranteed in any finite region of the state space. Since the unmodeled but bounded dynamics of the system is systematically encapsulated in the system model, the only influence that this imposes on the stability is the respective bounds on the controller gains. The controller design strategy is simple

and practicable with low computation burden which makes it easy to apply for control of MEMS optical switch.

7. References

[1] Judy, J. W. 2001. Microelectromechanical systems (MEMS): fabrication, design and applications, Smart Mater. Struct., 10, 1115-1134.

[2] Lu, M. S. C. and Fedder, G. 2004. Position control of parallel-plate micro actuators for probe-based data storage, Journal of Microelectromech System, 13(5), 759-769.

[3] Vagia, M. and Tzes, A. 2007. Robust PID control design for an electrostatic micromechanical actuator with structural uncertainty, IET control Theory and Applications, 2(5), 365-373.

[4] Borovic, B., Hong, C., Liu, A. Q., Xie, L. and Lewis, F. L. 2004. Control of a MEMS optical switch, 43rd IEEE Conf. on Decision and Control, 3039-3044.

[5] Li, J., Zhang, Q. X. and Liu, A. Q. 2003. Advanced fiber optical switches using deep RIE (DRIE) fabrication, Sensors and Actuators A, 102(3), 286-295.

[6] Chen, R. T., Nguyen, H. and Wu, M. C. 1999. A high-speed low-voltage stress-induced micromachined 2x2 optical switch, IEEE Photonics Technology Letters, 11(11), 1396–1398.

[7] Sentura, S. D. 2000. Microsystems Design. Kluwer Academic Publishers.

[8] Park, J., Wang, L., Dawson, J. M., Hornak, L. A. and Famouri, P. 2005. Sliding mode-based microstructure torque and force estimations using MEMS optical monitoring. IEEE Sensors Journal, 5(3), 546-552.

[9] Torabi, K., Vali, M., Ebrahimi, B. and Bahrami, M. 2010. Robust control of Nonlinear MEMS optical switch based on quantitative feedback Theory, 5th IEEE International Conference on Nano/Micro Engineered and Molecular systems, 122-128.

[10] Ebrahimi, B. and Bahrami, M. 2006. Robust sliding-mode control of a MEMS optical switch. Journal of Physics, Conference Series., 34, 728–733.

[11] Fei, J. and Batur, C. 2007. A novel adaptive sliding mode controller for MEMS gyroscope, 46th IEEE Conference on Decision and Control, USA, 3573-3578.

[12] Borovic, B., Liu, A. Q., Popa, D., Cai, H. and Lewis, F. L. 2005. Open-loop versus closed-loop control of MEMS devices: choices and issues, J. Micromechanics, Microengineering, 15(10), 1917-1924.

[13] Owusu, K. O., Lewis, F. L., Borovic, B., and Liu. A. Q. 2006. Nonlinear control of a MEMS Optical Switch, Proceedings of the 45th IEEE Conf., on. Decision & Control, 597-602.

[14] Saif, M., Ebrahimi, B. and Vali, M. 2012. A second order sliding mode strategy for fault detection and fault-tolerant-control of a MEMS optical switch, Mechatronics, 22(6), 696-705.

[15] Goodarzi, M. 2015. Robust Lyapunov-based Control of MEMS Optical Switches, Journal of Modern Processes in Manufacturing and Production,4, 59–71.

[16] Hassani, A. and Khatamianfar. A. 2010. Robust control of a MEMS optical switch using fuzzy tuning sliding mode, International Conf. on. Control, Automation and Systems, 2281-2284.

[17] Sarraf, E. H., Cousins, B., Cretu, E., and Mirabbasi, S. 2011. Design and implementation of a novel sliding mode sensing architecture for capacitive MEMS accelerometers, J. Micromech. Microeng, 21, 1-14.

[18] Yazdi, N., Sane, H., Kudrle, T. D., and Mastrangelo. C. H. 2003. Robust sliding mode control of electrostatic torsional micro mirrors beyond the pull-in limit, Int. Conf. on Solid State Sensors, Actuators and Microsystems, 1450-1453.

[19] Kilbas, A., Srivastava, H. and Trujillo, J. 2006. Theory and applications of fractional differential equations, Elsevier.

[20] Utkin. V. I. 1978. Sliding modes and their applications to variable structure systems, MIR, Moscow.

[21] Utkin. V. I. 1984. Variable structure systems: present and future, Automation and Remote control., 44, 1105-1120.

[22] Yu, X., Man, Z. and Wu, B. 1998. Design of fuzzy sliding-mode control systems, Fuzzy sets and systems, 95, 295-306.